Int. J. Electrochem. Sci., 10 **(2015)** 6537 - 6547

International Journal of
ELECTROCHEMICAL
SCIENCE
www.electrochemsci.org

Effect of Aspect Ratio of Titanium Dioxide Nanotube Arrays on the Performance of Lithium Ion Battery

Tauseef Anwar[1], *Li Wang*[2], *Liang Tongxiang*[3,*], *Xiangming He*[2], *Rizwan Ur Rehman Sagar*[3], *Khurram Shehzad*[4]

[1]Beijing Key Lab of Fine Ceramics, Institute of Nuclear and New Energy Technology, Tsinghua University, Beijing 100084, P.R. China
[2]Institute of Nuclear and New Energy Technology, Tsinghua University, Beijing 100084, China
[3] State Key Lab of New Ceramic and Fine Processing, Tsinghua University, Beijing 100084, China
[3]Laboratory of Advanced Materials, Department of Materials Science and Engineering, Tsinghua University, Beijing 100084, China
[4]Department of information science and electronic engineering, Zhejiang University, Hangzhou 310027, China.
[*]E-mail: txliang@tsinghua.edu.cn

Received: 8 April 2015 / *Accepted:* 28 May 2015 / *Published:* 24 June 2015

The relationship between nanostructure of electrode and performance of lithium ion batteries is essential for achieving tunable lithium storage in lithium ion batteries (LIBs). For this purpose, controllable growth of vertically aligned TNAs are achieved at room temperature by anodic oxidation method. The aspect ratio of these TNAs increases linearly with the increase of two parameters, growth-time and applied-voltage. Furthermore, these controlled TNAs are utilized as anode material in LIBs and areal capacity of LIBs is increased with the increase of aspect ratio of TNAs. In this way, the aspect ratio of TNAs is not only controlled in the range of 20-170 but also adjustable areal capacity of TNAs is obtained in the range of 100 ~ 600 μA h cm^{-2}. The stable areal capacity is obtained up to 50th cycle, indicating long operating life of LIBs. Such LIBs of tunable areal capacity with the help of aspect ratio of TNAs herald a new paradigm for energy storage systems.

Keywords: Titanium dioxide nanotube arrays (TNAs), Aspect ratio, Lithium ion batteries (*LIBs*).

1. INTRODUCTION

The lithium ion battery (LIBs) is a promising energy storage device and a viable power source applied in all current portable electronic devices.[1, 2] The LIBs are becoming a hot research topic for scientist due to its high capacity and long life.[3] The LIBs performance depends largely on the

structures and properties of electrode materials for lithium storage.[4] New superior electrode materials with high capacity, high rate capability, excellent thermal and structural stability are required to replace conventional graphite anode.[5-8] To date, numerous oxide materials have been developed as they have higher specific capacity and volumetric energy density than that of commercial graphite anode.[4, 9-14] The titanium dioxide (TiO_2) among oxide materials have high potential window, low volume expansion (3%), low toxicity, environmental benignity and widespread availability made it a good option as an alternative anode material for LIBs.[9, 15, 16]

The anodic oxidation is the best approach to fabricate titanium dioxide nanotube arrays (TNAs) with vertically aligned orientation, uniform distribution and high specific surface area.[17] In addition, anodic oxidation provides additive-free electrodes, which could enhance the performance of LIBs.[18] The growth parameters could be optimized in anodic oxidation and electrochemical properties of lithium ion battery may also be tuned. Although many research groups are using TNAs as anode in LIBs, [9, 19, 20] still there is a need to understand the fundamental relationship between nanostructure of TNAs and LIBs performance.

Until now, there are rare reports about the relationship between aspect ratio of TNAs and LIBs performance.[21] Therefore, high aspect of TNAs fabricated through anodic oxidation is the need of the hour. The anodic oxidation method could be used to fabricate the TNAs with particular aspect ratio. The control over aspect ratio of TNAs may be useful to get control over the areal capacity of LIBs.

Herein, controlled growth of TNAs was achieved on a titanium substrate by anodic oxidation method. The aspect ratio of TNAs was tuned via growth time and applied voltage. The TNAs were utilized as anode material in lithium ion battery. The areal capacity of TNAs was correlated with aspect ratio for the first time. As aspect ratio improved with increasing time and voltage, the areal capacity also increases relatively.

2. EXPERIMENTAL DETAIL

2.1 Preparation of highly ordered TNAs

Prior to anodic oxidation, titanium foil (0.125 mm thick foil, 99.7% purity, Sigma Aldrich) was degreased by sonication in acetone, ethanol and deionized water in turn for about 10 min, then dried in air. The electrochemical cell for anodization was a two-electrode cell, consisted of Ti foil as working electrode and platinum foil as counter electrode. Electrochemical anodization experiments were conducted at a constant potential with a DC power supply (DH1722A-2 110V/3A). The electrolyte was 0.3 wt. % NH_4F and 2 vol. % water in ethylene glycol (99.8%, anhydrous). These all experimental steps were performed at room temperature. The pre-anodization (first anodization) was carried out at 50 V for 6 hours. Then the grown nanotubes (sacrificial layer) were removed by ultra-sonication in ethanol or acetone for few minutes which left foot prints behind at titanium substrate. Than the second anodization is carried out at different voltages of 20, 30, 40 and 50 V and different time from 30, 60, 90 and 120 minutes to find optimized parameters. After completion of second anodization, voltage is

increased swiftly to 110 V for 5 minutes to peel out nanotubes for further characterization. The peeled out nanotubes are dried at 105 °C overnight and annealed at 450 °C for 2 h to transform from the as-prepared amorphous-TNAs phase to anatase-TNAs phase.

2.2 Characterization

Field Emission Scanning Electron Microscopy (FESEM LEO 1530) was used for surface and morphological studies of specimens. X-ray diffraction (Rigaku-XRD) was utilized for phase identification in TNAs.

2.3 Electrochemical characterization

The electrochemical performances of TNAs were characterized using Li|TiO_2 half cells. The 2032 coin-type half cells were assembled in an argon filled glove box. The working electrode was a mixture of TNAs, conductive agent and binder with a mass ratio of 70:24:6 at copper foil as current collector. A celgard 2300 polypropylene separator soaked with a liquid electrolyte, which is 1 M $LiPF_6$ in a 1:1 volume ratio of ethylene carbonate (EC) and dimethyl carbonate (DMC). The cells were galvanostatically charged and discharged between 1.0 and 2.5 V (*vs*. Li/Li^+) at the rate of 0.1C.

3. RESULTS AND DISCUSSION

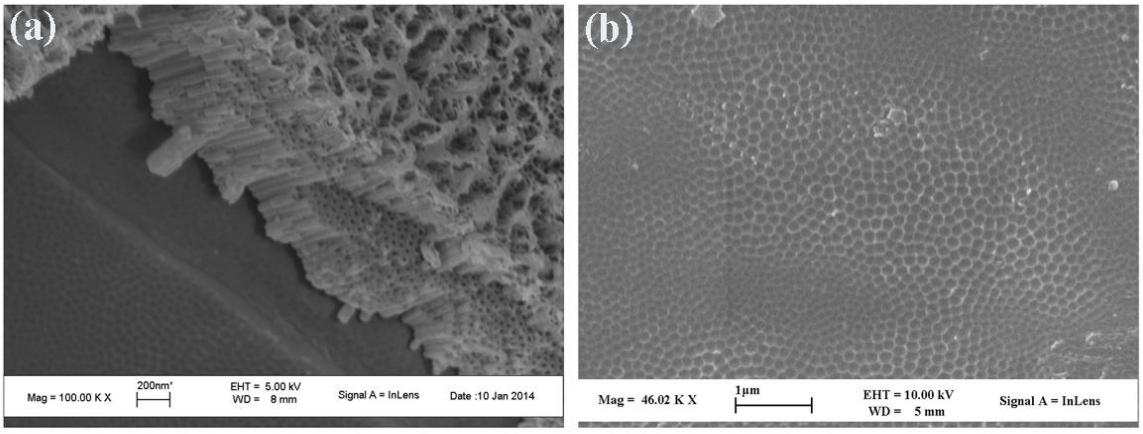

Figure 1. (a) The debris on the top of TNAs during first anodization. (b) The pits on the top of Ti-substrate after removal of TNAs.

The surface of as grown TNAs after first anodization was full of debris on the surface,[22-24] which was not only an issue during the growth of high quality TNAs but also hindered lithium ion intercalation and electron transport (Fig. 1 (a)).[25] Usually, ultrasonication has been adopted to remove debris, which cracked TNAs and surface of as grown TNAs was also affected. A method

adopted to overcome such a situation after completing first anodization. Firstly, grown TNAs were removed by ultra-sonication, which left regular hexagonally packed pits on Ti-substrate (Fig. 1 (b)).

The production of pits after first anodization on the titanium substrate is helpful to obtain debris free vertically aligned nanotubes. Thus, the growth of TNAs on Ti-substrate during second anodization was faster, more ordered in distribution and debris free due to the presence of a preformed pathway.

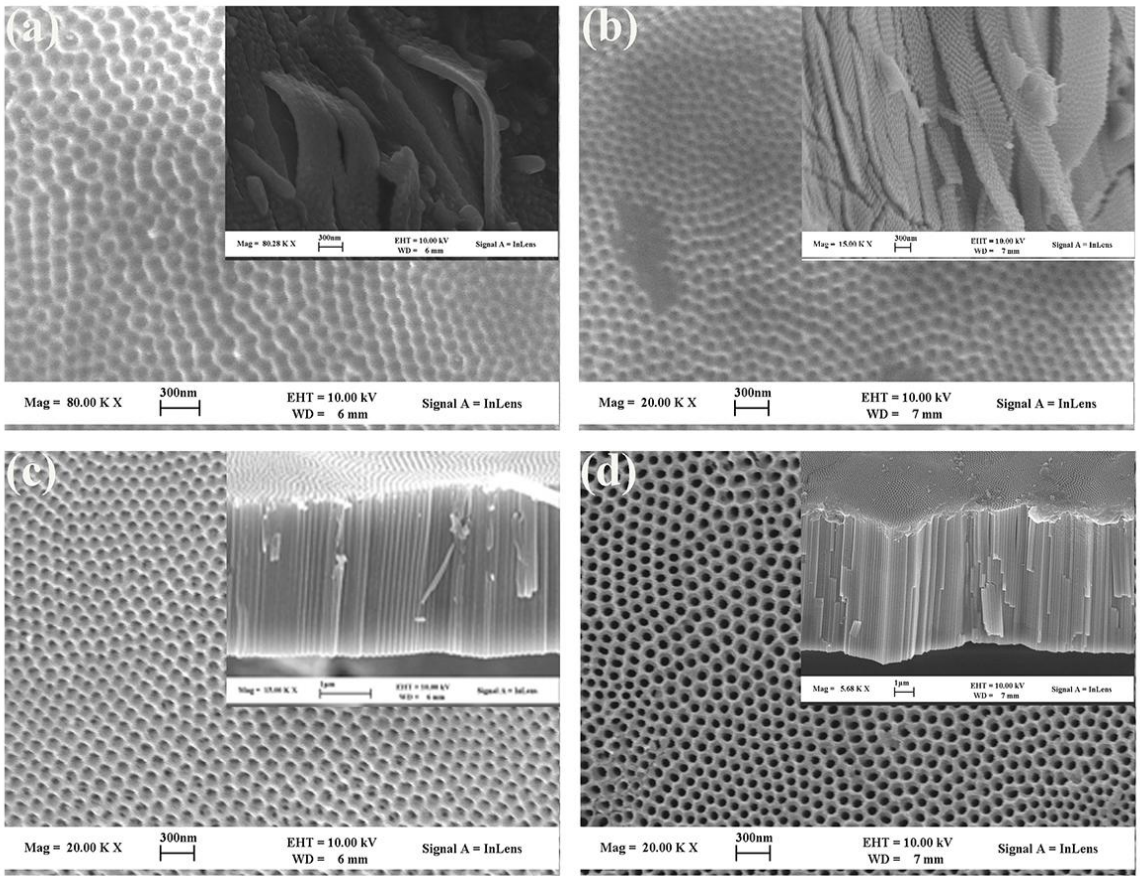

Figure 2. Top and lateral (inset) view of TNAs prepared at (a) 20 (b) 30 (c) 40 and (d) 50 V.

The lateral and top view of TNAs fabricated in the voltages range of 20-50 V at constant time duration of 2 h confirmed the growth of TNAs (Fig. 2). At the lowest voltages of 20 V, the growth process was very slow and only a thin layer was obtained with the shape of foot-prints (fig. 2 (a)). At the voltage of 30 V, the growth process was also slow and a thin layer with a little increase in thickness was formed and the pits were more prominent (Fig. 2 (b) and inset of Fig. 2 (b)). The TNAs synthesized at 40 V have shorter length nanotubular structure and top view indicated that the pores were not fully opened (Fig. 2 (c) and inset of Fig. 2 (c)). So the growth voltage was further increased to 50 V, due to which length of nanotubes increased and top surface was with open pores (Fig.2 (d) and inset of Fig. 2 (d)).

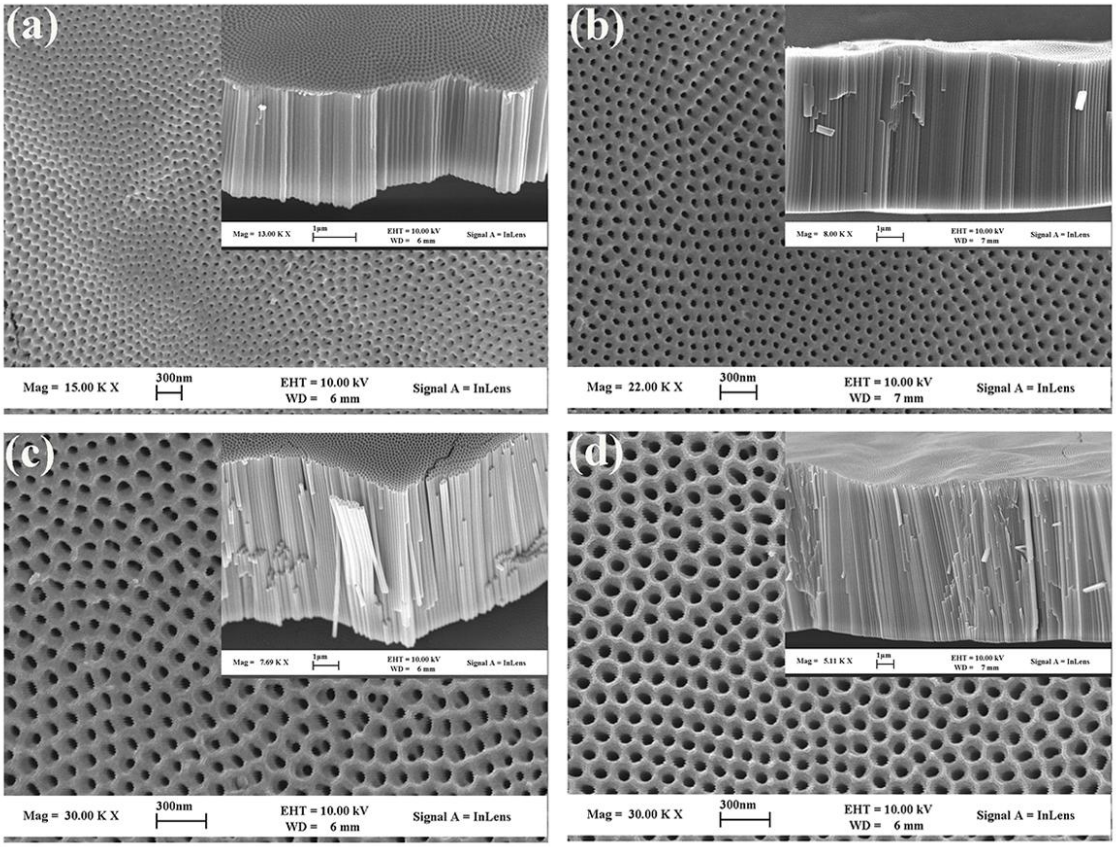

Figure 3. Top and lateral (inset) view of TNAs fabricated for (a) 30 (b) 60 (c) 90 and (d) 120 mins.

The growth of TNAs depends upon different parameters and time duration of anodic oxidation is an important parameter in the growth process. The fabrication time was also altered from 30-120 minutes, while applied potential was constant at 50 V (Fig. 3). The short length and small diameter of tubular morphology of TNAs was observed under 30 mins growth time duration (Fig. 3 (a) and inset of Fig. 3 (a)). As anodization time was increased from 30 mins to 60 mins, the length and pore diameter of TNAs were also increased (Fig. 3 (b) and inset of Fig. 3 (b)). The length increased further and pores were more opened at the growth time of 90 mins (Fig. 3 (c) and inset of Fig. 3 (c)). At the anodization of 120 mins, the increase in length of TNAs was at maximum in studied time range of 30 ~ 120 minutes (Fig. 3 (d)).

The length and diameter of TNAs could be estimated by using lateral and top view of SEM images**.** The increase of anodization time (30 ~ 120 mins) under a constant voltage of 50 V brought increase in diameter and the length of TNAs in the range of 23 ~ 47 nm and 2.44 ~ 7.84 μm, respectively (Fig. 4 (a)). The increase in the voltage (20 ~ 50 V) under constant growth time 120 mins brought an increase in the inner diameter and length of TNAs in the range of 33 - 47 nm and 0.19 - 7.84 μm, respectively (Fig. 4 (b)). In addition, the aspect ratio of TNAs was calculated by dividing length to diameter of TNAs and the highest aspect ratio of 170 was obtained.

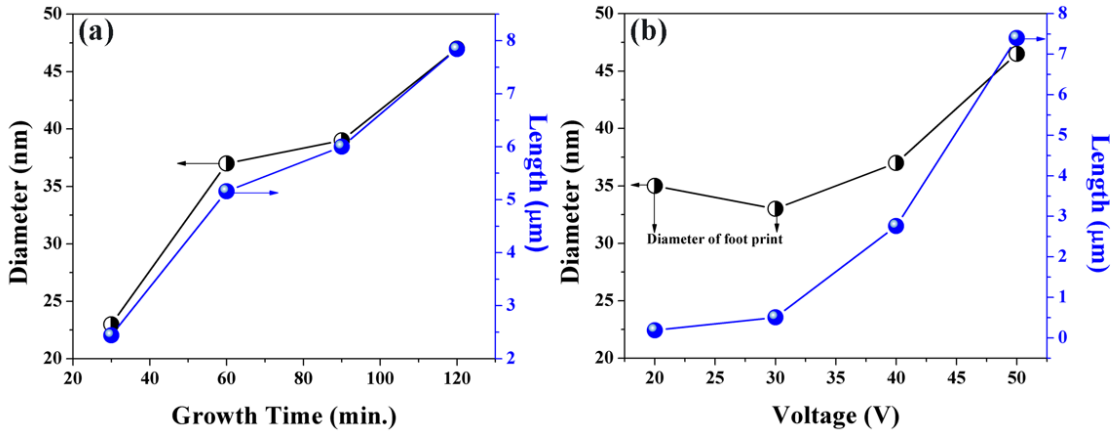

Figure 4. The diameter and length of TNAs fabricated at different (a) growth time and (b) voltage.

The crystallographic structure of titanium (substrate), as-prepared TNAs and annealed TNAs were investigated by powder X-ray diffraction (Fig. 5). The XRD patterns of Ti-substrate showed peaks that indicated polycrystalline nature of substrate. The as-prepared TNAs by anodic oxidation did not show any diffraction peak depicted that as-prepared TNAs were amorphous. The amorphous TNAs were transformed into anatase TNAs after annealing at 450 ^{o}C under air atmosphere.

The diffraction patterns revealed the formation of anatase polycrystalline structure (JCPDS 21-1272). When the annealing temperature is higher than 500 °C, titanium substrate itself oxidized to produce rutile TiO_2 layer which produce protrusion. The protrusion disturbed nanotube structure and accelerate phase transformation from anatase to rutile phase. As TNAs were peeled off from substrate, so there is no chance of protrusion and phase is 100% anatase.

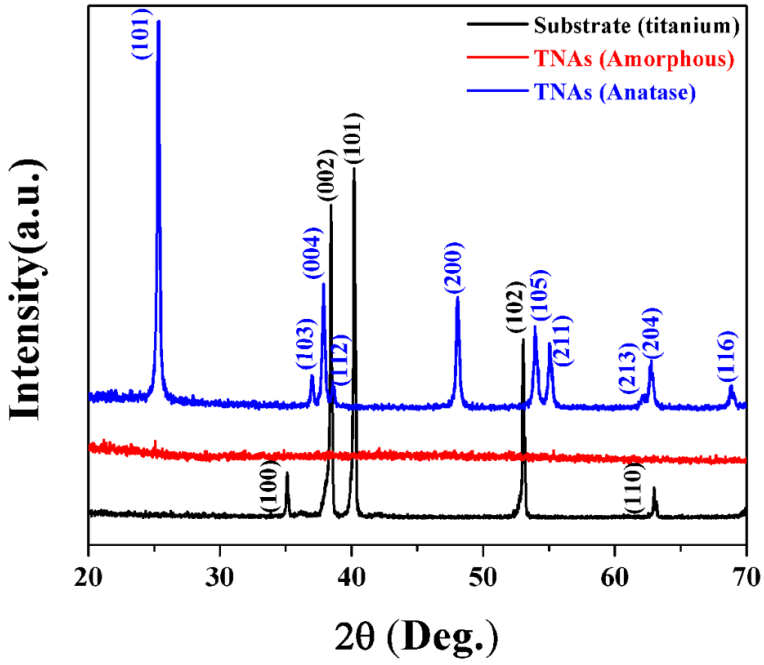

Figure 5. XRD patterns of Ti-substrate and amorphous, anatase TNAs.

These TNAs were used as anode material in lithium ion batteries (LIBs). The Li^+ insertion and extraction in TiO_2 electrode can be written as:[26]

$$TiO_2 + xLi^+ + xe^- \leftrightarrow Li_xTiO_2 \quad (1)$$

The lithium insertion coefficient is different for different morphologies and phases of TiO_2, for example, it is ~0.5 for anatase, ~1 for amorphous and ~1 for TiO_2 (B). [10-12] The first three charge and discharge curves are shown in fig. 6 (a) and (b) for the amorphous and anatase-TNAs electrodes between the potential window of 1 to 2.5 V. For amorphous-TNAs, the Li^+ insertion and extraction could be deduced from sloping curve. The voltage plateau of amorphous-TNAs was not observed during the insertion and extraction of lithium ions. The amorphous-TNAs contained large amount of disordered structures and defects, which provide spaces for lithium ions insertion homogeneously at relatively higher potential and without the feature of a two-phase reaction between Li_xTiO_2 and TiO_2.

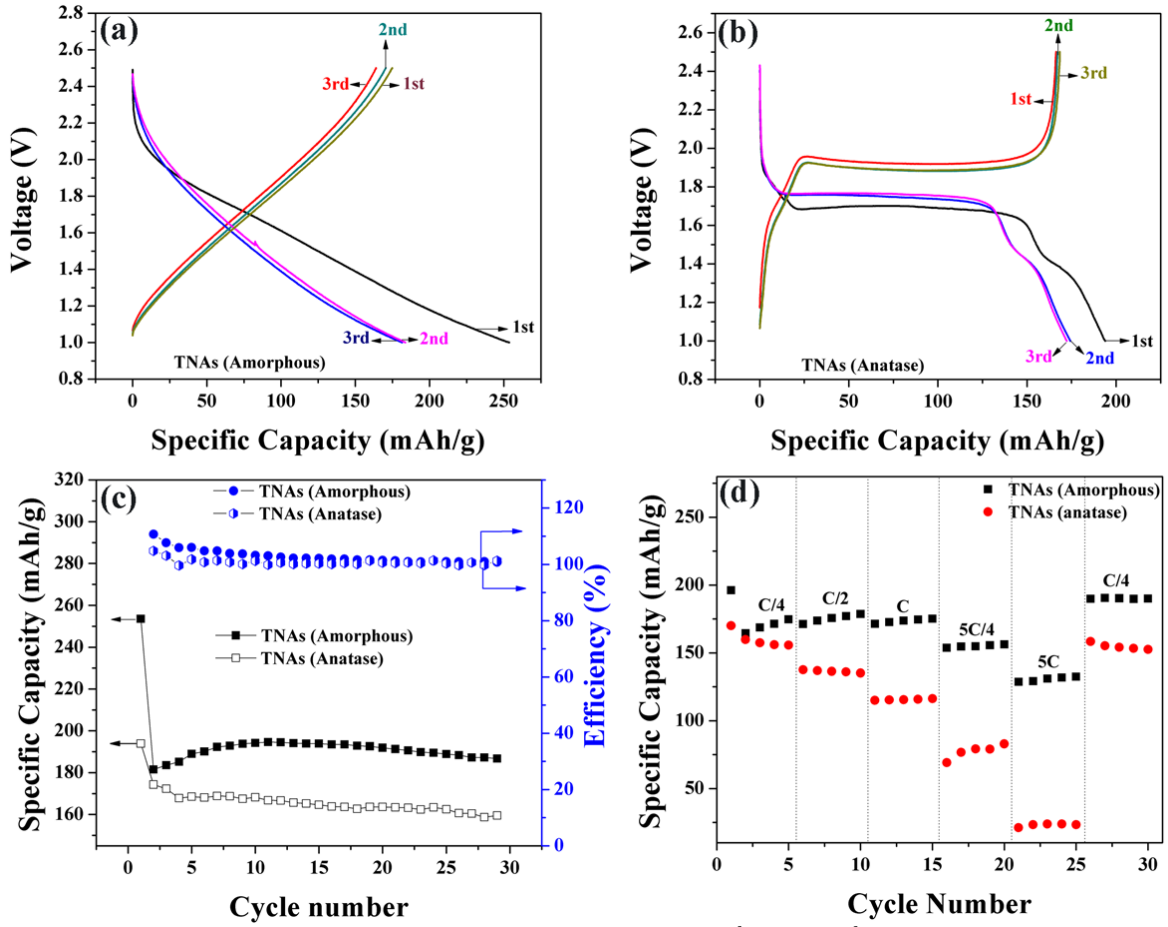

Figure 6. Electrochemical characterization (a) The 1st, 2nd and 3rd charge/discharge profiles of amorphous-TNAs at 0.1 C. (b) The 1st, 2nd and 3rd charge/discharge profiles of anatase-TNAs. (c) Cycle performance and coulombic efficiency at 0.1 C. (d) Comparison of rate capability between amorphous-TiO_2 nanotube arrays and anatase-TiO_2 nanotube arrays.

In contrast to amorphous-TNAs, the voltage plateaus were observed in the charge/discharge curves for anatase-TNAs electrode, due to Li^+ insertion and extraction from tetrahedral and octahedral sites, respectively. The discharge capacity (253 mAh/g) of the amorphous-TNAs was superior to that

of the anatase-TNAs (194 mAh/g), indicating accommodation of higher lithium per TiO_2 (x ≈1) in amorphous-TNAs compared to anatase (x ≈ 0.5). The irreversible capacity of amorphous-TNAs (24 %) was found higher than that of anatase-TNAs (10 %) in the first discharge cycle. This difference is the result of structural and chemical defects existing Li^+ traps in amorphous TNAs.

The stable cycle performance and 100 % coulombic efficiency was observed in both amorphous and anatase-TNAs (Fig. 4 (c)). The efficiency of amorphous-TNAs was little higher than that of anatase-TNAs. The discharge capacity of the amorphous-TNAs electrode increased up to the 10^{th} cycle probably due to the electrode surface activation. While the discharge capacity of anatase-TNAs became stable after few cycles and remained stable in the following cycles.

The rate performance at various discharge rates C/4, C/2, C, 5C/2, 5C and C/4 were observed (Fig. 6 (d)). The increment in discharge rate resulted into the increase of the difference in specific discharge capacity of amorphous and anatase-TNAs. When the discharge rate was again at C/4, the capacities for both amorphous-TNAs and anatase-TNAs were better than the previous. This might be attributed due to the reforming of the surface and bulk structure during charge/discharge. Moreover, the low rate capability was observed in anatase-TNAs as compared to amorphous.

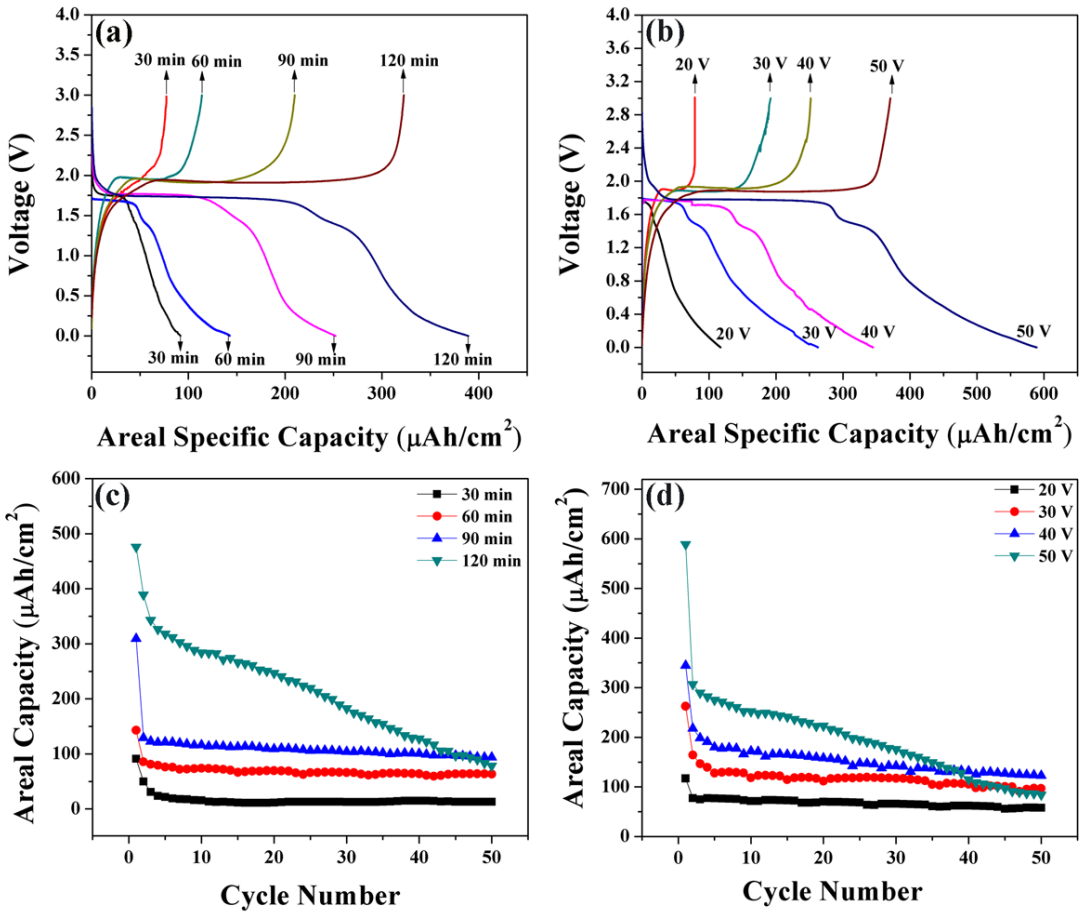

Figure 7. The 1st charge/discharge curves at the current density of 10 μA cm^{-2} for different (a) growth time and (b) applied voltage. The cycling performance of TNAs fabricated for different (c) growth time and (d) applied voltage. The first two cycles were measured at the current density of 10 μA cm^{-2} and remaining cycles are at 50 μA cm^{-2}.

There are several issues regarding the measurement of gravimetric specific capacity. Firstly, the inhomogeneous blending of the additives (polymeric binders and conductive materials) and electroactive materials influenced the diffusion paths of lithium ions and electrons in the electrode. Secondly, gravimetric specific capacity needed a specific amount, which requires a lot of efforts. Thirdly, for gravimetric specific capacity needed peel off of TNAs, which is impossible in the case of thin TNAs layer. So additive-free electrodes were required to elucidate the correlation between the electrochemical performance and structural properties of TNAs. Therefore, we used as grown samples of TNAs as electrode in half cells annealing at 450 ^{o}C and obtained the areal capacity.

The areal capacity was measured to avoid above-mentioned issues in the measurement of gravimetric specific capacity. The areal specific capacity of 1st charge/discharge for TNAs fabricated at 30, 60, 90 and 120 mins was obtained around of 92, 142, 309 and 497 µA h cm^{-2}, respectively (Fig. 7 (a)). Similarly, the areal specific capacity of TNAs fabricated at different voltage of 20, 30, 40 and 50 V was 117, 263, 345 and 590 µA h cm^{-2}, respectively (Fig. 7 (b)). The areal specific capacity of fabricated TNAs was increased accordingly, as the growth parameters (time duration and voltage) were increased. The cycling performance of TNAs grown at different time duration (Fig. 7 (c)) and applied voltage (Fig. 7 (d)) depicted that controlled growth time and voltage could tune cyclic performance. So the electrochemical performance could be tuned according to the requirement.

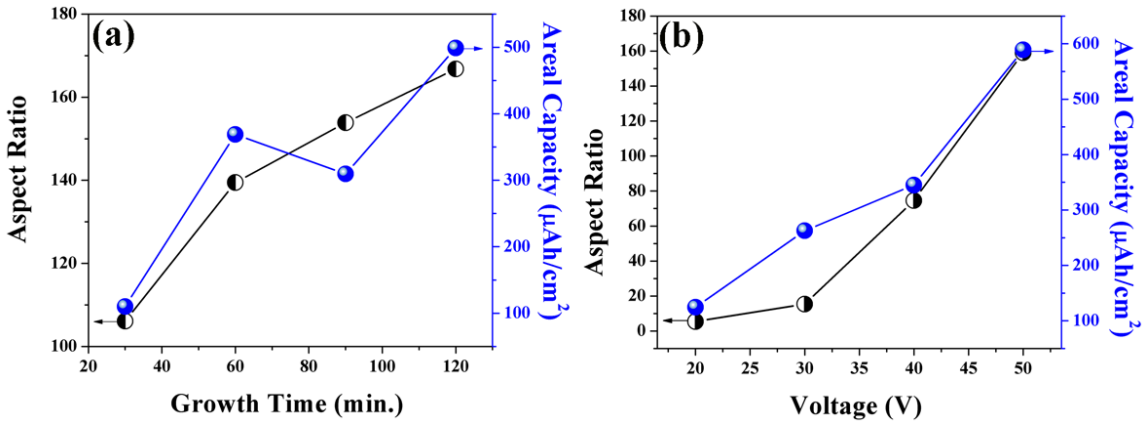

Figure 8. Change in aspect ratio and areal capacity with respect to (a) growth time and (b) voltage.

The areal capacity of TNAs was increased with the increase of aspect ratio of TNAs. The highest areal capacity of 600 µA h cm^{-2} was achieved at absolute aspect ratio of 170 (Fig. 8). In this way, tuning of growth time resulted into a tunable aspect ratio and this tuned aspect ratio tuned the areal capacity (Fig. 7 (a)). In the similar fashion, applied voltage was varied under a constant time of 120 mins, which resulted into a tunable aspect ratio of TNAs (Fig. 8 (b)). This tuned aspect ratio again tuned the areal capacity of LIBs. Thus, we are able to establish a relationship between aspect ratio and the areal capacity of LIBs. The increment in the length of TNAs increased the areal capacity of LIBs. The distance covered by Li-ions after inserting into the anode material might have played a major role in the areal capacity of LIBs. Therefore, higher aspect ratio represents higher length of TNAs, which

resulted in higher areal capacity. Thus, tunable areal capacity might be the result of large Li-atoms path into the long TNAs.

Tang et al.[21] achieved high performance and long life LIBs by tuning the aspect ratio of titanium dioxide nanotubes. They claimed this report was first in its nature. They used hydrothermal method to synthesis titanium dioxide nanotubes. The hydrothermal synthesis process have demerits in terms of high growth temperature and non-vertical nanotubes. On the other hand anodic oxidation could produce vertical nanotubes arrays at room temperature. Therefore, our study may be useful for further high performance of LIBs.

4. CONCLUSIONS

The growth of aligned TNAs is achieved by controlling the anodic oxidation parameters, such as applied voltage and time. The resulted aligned TNAs presented inner diameter and length in the range of 10 ~ 50 nm and 0.2 ~ 7.84 μm, respectively. The as-prepared TNAs are amorphous, and these are proved to transform into anatase phase without change in morphology by annealing treatment at 450 ^{o}C. The amorphous-TNAs shows higher lithium storage capacity, lower over potential and better rate capability comparing with the anatase-TNAs, being more favorable for the lithium ion batteries. The amorphous-TNAs exhibit reversible capacity of 253 mAh g^{-1} and remain constant even after 30 cycles, indicative of good cycleability. The areal capacity of these TNAs is tuned in the range of 90 ~ 600 μA h cm^{-2} by tuning the aspect ratio. Our study not only provided a systematic study of tunable TNAs but we are also able to obtain tunable areal capacity that is necessary for the better performance of LIBs.

ACKNOWLEDGEMENTS

This work is supported by the National Natural Science Foundation of China (Grand No. 21271114); Tsinghua University independent research and development fund (20111080982) and Program for Changjiang Scholars and Innovative Research Team in University (IRT13026)

References

1. T. Sasaki, Y. Ukyo and P. Novák, *Nat Mater*, 12 (2013) 569.
2. J.M. Tarascon and M. Armand, *Nature*, 414 (2001) 359.
3. M. Armand and J.M. Tarascon, *Nature*, 451 (2008) 652.
4. S. Goriparti, E. Miele, F. De Angelis, E. Di Fabrizio, R.P. Zaccaria and C. Capiglia, *J. Power Sources*, 257 (2014) 421.
5. N. Nitta, F. Wu, J.T. Lee and G. Yushin, *Mater. Today*
6. W. Yang, W. Jiaping, J. Kaili and F. Shoushan, *Front. Phys*., 9 (2014) 351.
7. J.H. Jeong, D.W. Jung and E.S. Oh, *J. Alloys Compd.* , 613 (2014) 42.
8. L.W. Xiangming He, Weihua Pu, Guoyun Zhang, Changyin Jiang, Chunrong Wan, *Int. J. Electrochem. Sci.*, 1 (2006) 12.
9. X. Su, Q. Wu, X. Zhan, J. Wu, S. Wei and Z. Guo, *J Mater Sci*, 47 (2012) 2519.
10. P. Roy and S.K. Srivastava, *J. Mater. Chem.* A, 3 (2015) 2454.

11. Y. Deng, L. Wan, Y. Xie, X. Qin and G. Chen, *RSC Advances*, 4 (2014) 23914.
12. L. Zhang, H.B. Wu and X.W. Lou, *Adv. Energy Mater.*, 4 (2014) n/a.
13. M.V. Reddy, G.V. Subba Rao and B.V.R. Chowdari, *Chem. Rev.* , 113 (2013) 5364.
14. B. Liu, A. Abouimrane, M. Balasubramanian, Y. Ren and K. Amine, *J. Phys. Chem. C*, 118 (2014) 3960.
15. Q.H. Tian, J.Z. Song, Z.X. Zhang, L. Yang and S. Hirano, *Mater. Chem. Phys.* , 151 (2015) 66.
16. Z.C. Yan, L. Liu, J.L. Tan, Q. Zhou, Z.F. Huang, D.D. Xia, H.B. Shu, X.K. Yang and X.Y. Wang, *J. Power Sources*, 269 (2014) 37.
17. A. Lamberti, N. Garino, A. Sacco, S. Bianco, D. Manfredi and C. Gerbaldi, *Electrochim. Acta* 102 (2013) 233.
18. J. Jiang, Y. Li, J. Liu and X. Huang, *Nanoscale*, 3 (2011) 45.
19. N.A. Kyerematen*g*, *ChemElectroChem*, 1 (2014) 1442.
20. D. Guan, J. Li, X. Gao and C. Yuan, *RSC Advances*, 4 (2014) 4055.
21. Y. Tang, Y. Zhang, J. Deng, D. Qi, W.R. Leow, J. Wei, S. Yin, Z. Dong, R. Yazami, Z. Chen and X. Chen, *Angewandte Chemie International Edition*, 53 (2014) 13488.
22. B. Samran, P. Krongkitsiri, S. Pimmongkol, S. Budngam and U. Tipparach, Preparation and Microstructure of Titania (TiO2) Nanotube Arrays by Anodization Method, in: J. Nukeaw, W. Pecharapa (Eds.) *Advances in Material Science and Technology*, 2013, pp. 104.
23. C. Chien-Chon, C. Hsien-Wen, C. Chin-Hsing, L. Hsueh-Pei, L. Chi-Ming, C. Si-Fan, L. Liyang, H. Chen-Shiung and E.W.G. Diau, *J. Phys. Chem*. C, 112 (2008) 19151.
24. K. Shankar, J.I. Basham, N.K. Allam, O.K. Varghese, G.K. Mor, X. Feng, M. Paulose, J.A. Seabold, K.-S. Choi and C.A. Grimes, *J. Phys. Chem*. C, 113 (2009) 6327.
25. M.D. Ye, X.K. Xin, C.J. Lin and Z.Q. Lin, *Nano Lett.* , 11 (2011) 3214.
26. P. Suresh Kumar, V. Aravindan, J. Sundaramurthy, V. Thavasi, S.G. Mhaisalkar, S. Ramakrishna and S. Madhavi, *RSC Advances*, 2 (2012) 7983.

© 2015 The Authors. Published by ESG (www.electrochemsci.org). This article is an open access article distributed under the terms and conditions of the Creative Commons Attribution license (http://creativecommons.org/licenses/by/4.0/).